Electrical Bioimpedance Based Estimation of Diabetics

Pedro Bertemes-Filho

Abstract The improvement of life quality of diabetic patients requires periodic measurements of blood glucose, such as those affected by Diabetes Mellitus. They need to put a blood droplet on a dispensable reagent strip to measure the blood glucose level. Currently available devices for this purpose are invasive, in-involving painful, non-hygienic, and expensive measurement methods. Non-invasive devices, such as those using near-infrared (NIR), intend to be an alternative even though considered a low precision method compared to biochemical ones. Despite that, the creation of computational models to improve the precision of non-invasive blood glucose monitors combining multiple non-invasive technologies has recently been investigated, such as the use of electrical bioimpedance (BIA) data. BIA has been successfully used for cancer diagnosis and biomaterial characterizations due to its safety, low cost, effectiveness, portability, and applicability. The technique measures the impedance spectra of the material under study and then obtains its biological properties using a fitting model. This book brings the physical concepts of the BIA technique, including hardware and modeling for characterization. It also discusses the most reliable and promising applications for detecting blood glucose levels, both invasive and non-evasively. The usability, accuracy, precision, and performance of using the BIA approach are assessed and focused on diabetic diagnosis.

Keywords Blood glucose · Diabetes mellitus · Invasive · NIR · Electrical bioimpedance

1 Electrical Bioimpedance: Physical Concepts

The opposition flowing sensed by an electrical current across any biological material can be defined as bioimpedance (BIA, where "A" stands for analysis). It can be extended to DC (direct current) or AC (alternate current) applications. Generally, if the application involves the characterization of biomaterial, for example, tissue, then

P. Bertemes-Filho (✉)
Universidade do Estado de Santa Catarina, Joinville, Santa Catarina, Brazil
e-mail: pedro.bertemes@udesc.br

an impedance spectrum is required (i.e., electrical bioimpedance spectroscopy—EBS).

To better describe the physical concepts on bioimpedance, the previous basic definition of electrical impedance comes to be essential to establish. The impedance Z was defined by Georg Simon Ohm in Ohm's law in 1827, where Z ($=V/I$) is a complex number. It was only in 1893 that Arthur Kennelly represented it in terms of a real (R) and imaginary part (jX) [1], where $Z = R + jX$ and "j" is the imaginary operator. The difficulty of the materials produces the real part to DC flow (resistance), and the imaginary part (reactance) is produced by the combination of the self-induction of voltages in conductors by the magnetic fields of currents (inductance) and the electrostatic storage of charge induced by voltages between conductors (capacitance) [2].

When it comes to biological materials, many other variables may modify the electrical bioimpedance, such as sample shape, internal structure or chemical composition, sample moisture, and temperature [3]. Tissue can be represented by cells suspended in an extracellular fluid composed of 20% plasma and 80% interstitial fluids [4]. A single cell contains a lipid layer for mainly ion transport and protection. A cell membrane can be modeled as a capacitor parallel with a resistor. If we consider intra-cellular and extracellular mediums as uniform and isotropic, they can be modeled as simple resistors, as shown in Fig. 1. At lower frequencies and due to the unique isolating property of the cell membrane, R_m can be considered much higher than R_{ext}. The reactance generated by the membrane capacitance C_m is high. This effect impedes the ionic current from penetrating the cell, forcing the current
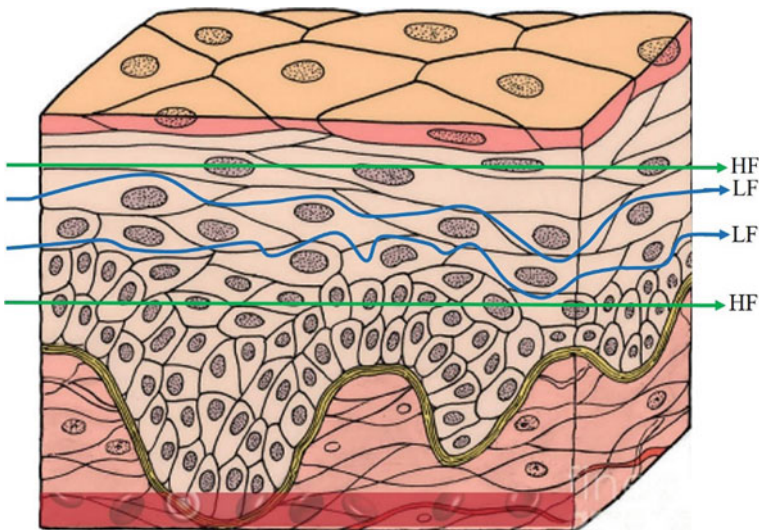

Fig. 1 Illustration of the ionic current flow across a type of skin tissue at lower (blue lines) and higher (green lines) frequencies

Fig. 2 Equivalent electrical circuit for a single cell, where R_{ext} represents the resistance of extracellular medium, R_m and C_m represents the cellular membrane resistance and capacitance, respectively, and R_{int} represents the resistance of the intracellular medium
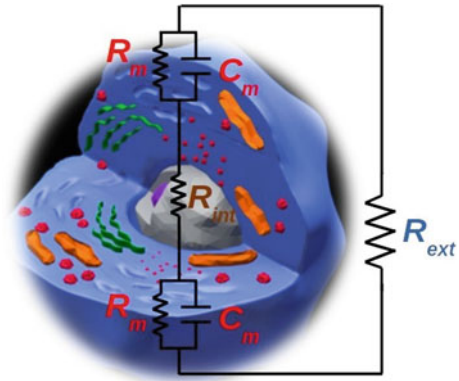
flow through the extracellular medium. On the other hand, the membrane reactance decreases at higher frequencies, allowing ionic current flow inside the cell [5].

Figure 1 brings a typical illustration showing how the cells interact with the electrical field at both low (blue lines) and high frequency (green lines). This mechanics permits calculating the impedance changes in tissue which, in turn, is used for characterization and then differentiating a normal tissue from a cancerous one, for example [6]. Characterization of biological samples can only be possible by fitting the measure impedance data into a proper electrical equivalent model, where sample properties are extracted [7].

The electrical equivalent model presented in Fig. 2 is just a simple data representation. However, bioimpedance is a complex number that also includes anisotropy and inhomogeneities. Therefore, it cannot be modeled with simple electrical components such as resistors (R) and capacitors (C), even if many RC models are connected in series or parallel. The electrical extraction properties of the biomaterial under study require the use of non-linear equations expressed in terms of fractional polynomials, such as the one suggested by [7]. The Cole equation has been widely used for tissue characterization over the last 50 years, where "α" (*alpha*) is a number from 0 and 1, ω_C is the cutoff frequency of the material, R_0 ($=R_{ext} + R_{int}$, assuming $R_m \gg R_{ext}$ and $R_{ext} \gg R_{int}$) and R_∞ ($=R_{ext}//R_{int}$,) where "//" denotes a parallel operation) represents the impedance at the lowest and highest frequency, respectively. Each biological material has its alpha value, which best describes the dispersion behavior of the electrical field inside of it. Table 1 brings the alpha values for a few biologically important materials. A more detailed list of such alpha values can be found in [8]. Equation 1 represents just a single-dispersion, but two Cole models can also be connected in series for studying wide frequency range applications of multiphase materials, such as blood, bovine milk, cancerous tissue, etc.

$$Z_{biol} = R_0 - \frac{R_0 - R_\infty}{1 + (j\omega/\omega_C)^{1-\alpha}} \tag{1}$$

Examples of biomaterial characterizations are shown in Fig. 3, where constant

Table 1 Cole-Cole alpha parameters obtained from approximately 10 Hz to 20 GHz [8]

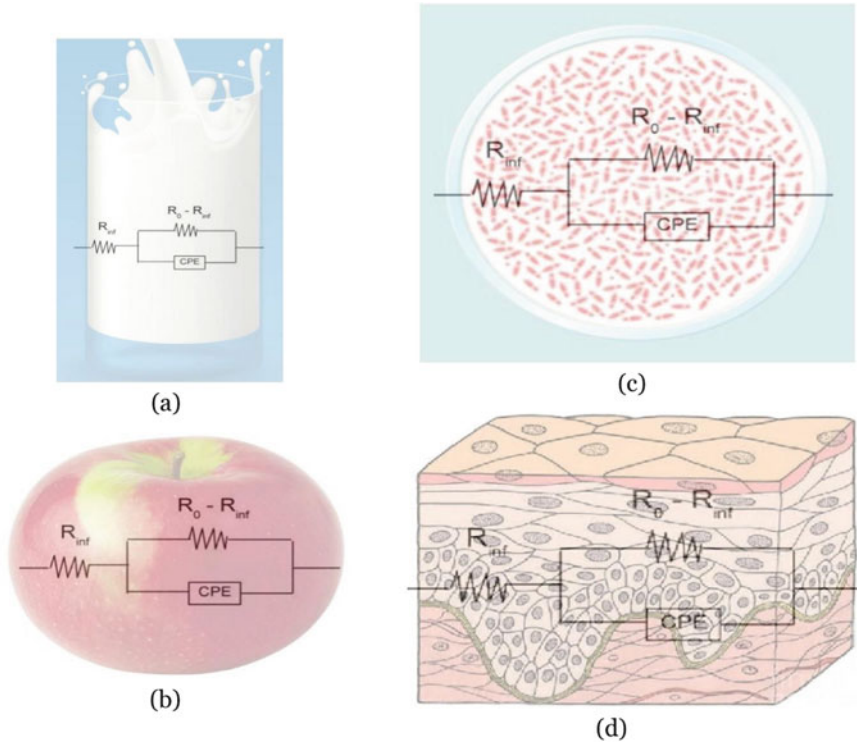| Tissue	f_C (kHz)	Alpha
Liver	1120.0	0.219
Bladder	846.0	0.077
Blood	947.0	0.092
Muscle (transverse)	175.0	0.093
Stomach	3060.0	0.122
Nerve	53.0	0.251

Fig. 3 Different types of biomaterial complexity using BIA technique for characterization, where R_0 represents the resistance at the lowest measured frequency whereas R_{inf} represents the highest frequency one. **a** Bovine milk. **b** Apple fruit. **c** Bacteria culture. **d** Slab of skin tissue

phase element (CPE) is a special case of the general fractional component whose impedance Z_{CPE} is equal to $1/(s^\alpha C)$ in the s-domain, where C is the capacitance and α is its order. As a result, a phase angle ϕ_{CPE} ($= \alpha \pi/2$) can be calculated for each material type as it is constant at all frequencies, depending only on the α value.

It is known from impedance spectroscopy studies undertaken over the last 80 years that biological samples, especially tissue, have different dispersion to the applied electrical field according to the frequency of the alternate excitation signal. This is because of the different free ions within both extra- and intracellular fluid. At lower frequencies, the ionic potential created by the external excitation signal will facilitate the free ions' flowing. The cell membrane impedes this flow, resulting in a high impedance when the amount of extracellular fluids is very small in cancer tissue. On the other hand, at higher frequencies, the ionic current also flows through the cell membrane and its intracellular contents, decreasing the impedance for most cases.

It can be concluded from the interactions of different ions types within a biological material that bioimpedance spectroscopy can easily differentiate tissue types and biomaterial structures in a rapid, effective, and low-cost manner.

2   Basic Hardware Structures

Most BIA systems inject a sinusoidal current with a constant amplitude over a wide frequency range by two electrodes to the sample, measure the resulting voltage by the other two electrodes, and then calculate the transfer impedance. This is a so-called tetrapolar technique whose contact impedance can be neglected from measured data. Figure 4 the ionic equipotential lines created by injecting (+I) and sank (−I) current inside a tissue sample. For example, the tetrapolar technique gives more accurate

Fig. 4 Representation of the ion equipotential lines created by an alternate electrical excitation current
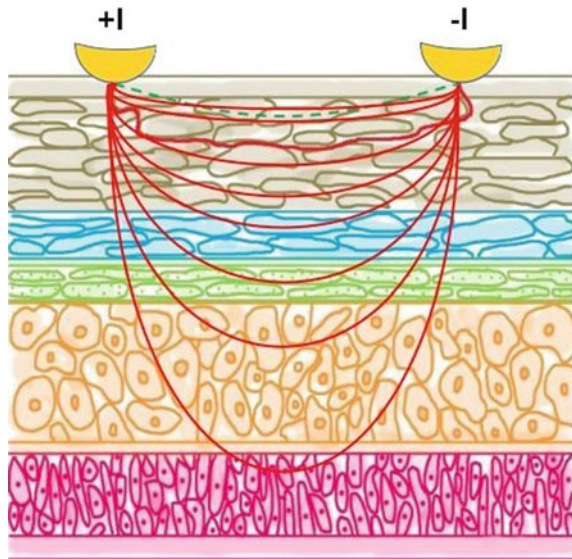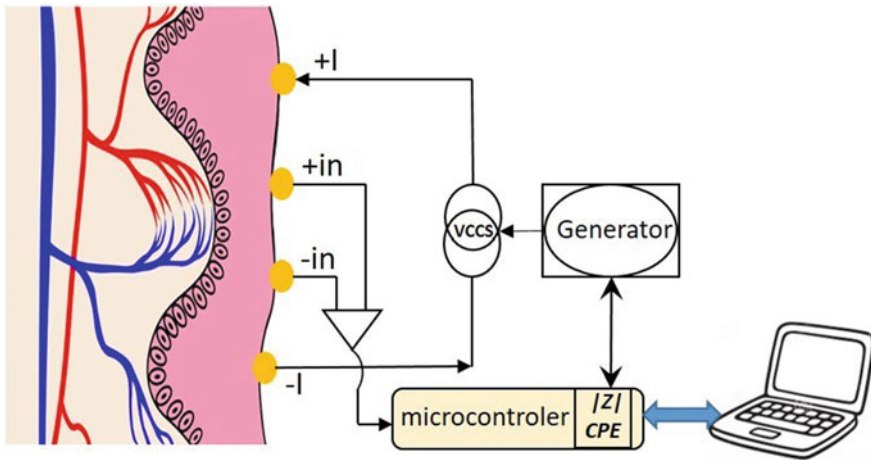
Fig. 5 Schematic diagram of a basic BIA hardware using the 4-electrode technique

information about the sample properties than the bipolar technique. However, electronic accuracy plays a great role in the measurements. All stray capacitance in the instrumentation, cables, and connectors degrades the BIA performance, especially at higher frequencies.

Blood analysis with BIA requires surface electrodes connected with minimal hardware, comprising mainly a current source and a front-end circuit. Figure 5 shows a hardware example for this application. The whole BIA setup can be built either as an all-in-one or a standalone system. A low-power microcontroller generates the signal and calculates both impedance modulus and phase. This type of system optimizes size and battery life by using low-cost integrated circuits (ICs), such as the AD5933 (Analog Devices, Inc., Norwood, MA), the AFE4300 (Texas Instruments Inc., Dallas, TX), the ADAS1000 (Analog Devices, Inc.) and the MAX30002 (Maxim Integrated, Inc., San Jose, CA). IC integrating bioimpedance meters contain the signal generator, excitation, and measuring circuits, including a small processor for calculating the impedance and doing the control interface.

A bioimpedance meter can easily be built from scratch either for in-vivo or in-vitro measurements by having some background in electronics. However, some commercial electrical impedance spectrometers (EIS) can also do in-vitro measurements. EIS is the standard device for measuring impedance in a frequency range. There is a wide range of manufacturers for these devices, such as Agilent, Zurich Instruments, HP, or Emerson. Commercial impedance analyzers may cost more than one thousand dollars, which can offer many tools to do impedance measurements such as high robustness to noise, high-quality layouts for high-speed signals, radiofrequency isolation, ultra-precise components for ultra-precise measurements, advanced measurements algorithms, and user-friendly software to make the measurements as much easy as possible.

In electronics, it is common sense that measuring impedance demands no more than applying Ohm's law, where a voltage is divided by a current. Therefore, low-cost devices have been increasing in this area over the last 10 years. A well-known low-cost device used for BIA measurements is the integrated circuit from analog devices AD5933 [9–12]. This device can do impedance measurements up to 300 kHz and cost no more than $60. On the other hand, it uses a bipolar technique, and it can perform measurements over 300 kHz if required. This is why most BIA designers prefer to build custom BIA hardware from scratch. In addition, a customized BIA gives the researcher more flexibility and efficiency in terms of hardware, signal processing, and applications.

It is important to mention that the flexibility and freedom while constructing custom instruments can be a drawback for standardization. The number of combinations when building a BIA hardware can be enormous and may be impossible to resume. An example of a simple BIA hardware is shown in Fig. 6, where current is injected through the connectors shown in Fig. 6d and voltage across the tissue is measured between the connectors shown in Fig. 6e.
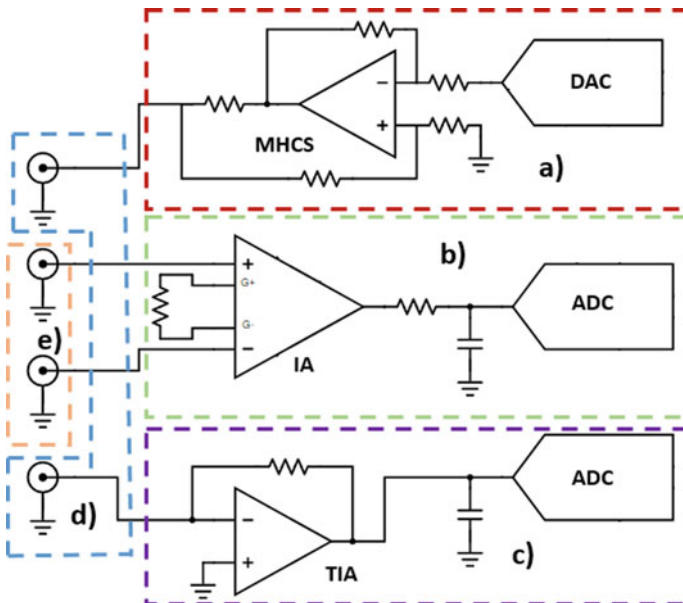

Fig. 6 Schematic diagram of a typical BIA hardware. **a** Current generator. **b** Voltage meter. **c** Current meter. **d** Current generator and current meter connections. **e** Voltage meter connections

2.1 Current Excitation Circuit

The current generation shown in Fig. 6a is divided into a digital to analog converter (DAC) and a voltage-controlled current source (VCCS). A DAC is a voltage source that may not be embedded into a Digital Signal Processor (DSP). DAC allows generating different shapes of a single frequency and multi-frequency waveforms, such as sine wave, sawtooth, triangle, or square. If multifrequency waveforms are used, some of the most common for BIA are multisine, Discrete Interval Binary Sequence (DIBS), or Maximum Length Binary Sequence (MLBS) [13]. VCCS is used to convert the voltage output from the DAC into the current injected into the tissue. The VCCS shown in figure x5 is well-known in the bioimpedance field, such as the modified Howland current source (HCS). Prof. Bradford Howland firstly proposed this source in 1962, published by [14] and modified by [15]. The modified HCS has been widely used in bioimpedance due to its simplicity, stability, high bandwidth [16, 17], and high output impedance [18].

Most BIA system uses a modified Howland current source (MHCS) with the grounded load. For the academic purpose and better understanding, we describe a proposed blood analysis design here, as shown in Fig. 7. The inverting input is fed by a binary signal supplied by the microcontroller ($V_{I/O}$). In contrast, the non-inverting input is biased with a trimmer voltage of 1.66 V to cancel the output current offset produced by the microcontroller signal. According to the transfer function of the MHCS shown in Eq. 2, $I_{out} = Z_4*(V_{1.66} - V_{I/O})/Z_5$ assuming $R_2 = R_3 = R_4 = R$ and $R_1 = R + R_5$ [18]. For example, if the input voltage $V_{I/O} = 3.3$ Vp and $R_5 = 3.3$ kΩ, the MHCS will produce an output current I_{out} of 1 mAp. The capacitor C_2 blocks DC currents coming from the MHCS, then avoiding DC currents flowing to the patient and preventing DC feedback to input, whereas C_1 prevents oscillations at higher frequencies.
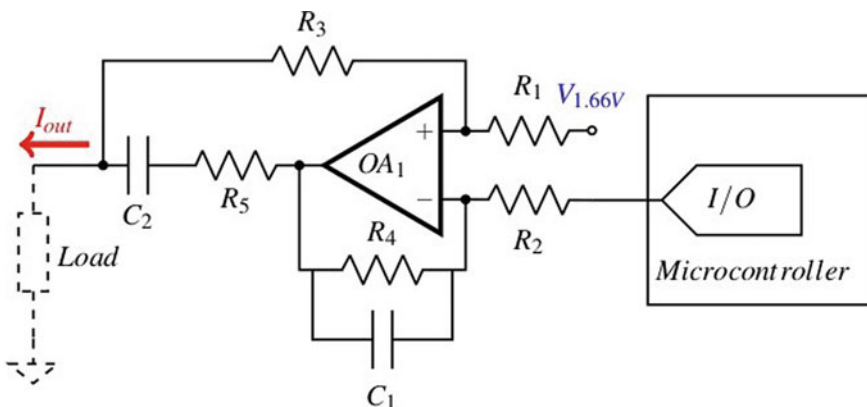

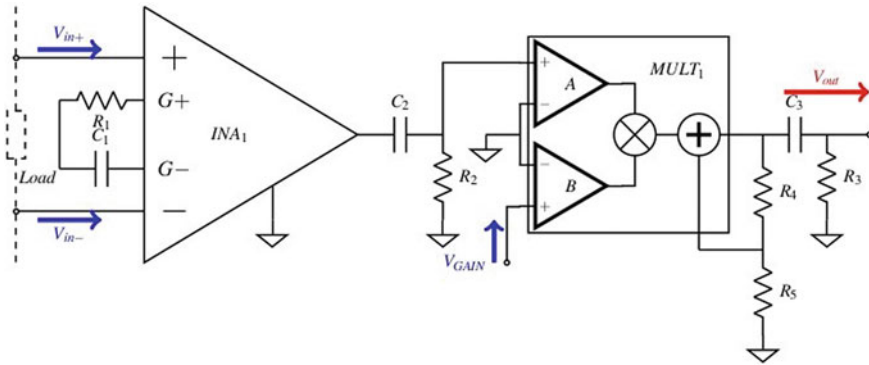**Fig. 7** Proposed current source for bioimpedance analysis of blood

Fig. 8 Basic voltage acquisition system for a typical BIA hardware

$$I_{\text{out}} = \left[\frac{R_1 \cdot Z_4 - R_2 \cdot R_3 - R_2 \cdot Z_3}{R_2 \cdot Z_5 - (R_1 + R_3)} \right] * V_{1.66} - \frac{Z_4}{R_2 \cdot Z_5} * V_{I/O} \qquad (2)$$

2.2 Voltage and Current Meters

Most of the acquisition systems used an Instrumentation Amplifier (IA), as shown in Fig. 8. This type of amplifier has a differential input and a single-ended output. It offers a high input impedance, high Common Mode Rejection Ratio (CMRR), and low DC offset. Usually, an IA feeds an Analog to Digital Converter (ADC) through a low-pass filter to digitize the analog signal.

Filtering is most often performed to remove unwanted signals and most types of noise from the data. The most common form of filtering is the low-pass one, which limits the bandwidth of the data by eliminating signals and noise above the filter's corner frequency. For example, the importance of low-pass filtering appears when the goal is to avoid the 50/60 Hz inference from the power supply. ECG, EMG and EEG biosignals usually apply this technique for rejecting the 50/60 Hz. In the case of Fig. 8, V_{out} is expected to be a DC value as a function of the impedance modulus, and then the AC component of the measured signal is removed by filtering it out.

Nonetheless, it is important to ensure that the ADC sample rate is at least double the maximum frequency generated by the DAC, guaranteeing the fulfillment of the Nyquist theorem.

A practical example of a voltage acquisition system is shown in Fig. 8. The instrumentation amplifier INA1 performs the differential voltage across the load at the first stage. The IA should be chosen according to the load properties and frequency range that best suits the characterization required. High input impedance, high voltage gain, and low output and input noise are highly recommended. As shown in Fig. 8, R1 and C1 form a high-pass filter for preventing the amplification of any DC signals

and then saturation of the *INA* output due to that signals. Before connecting the *INA* output to other signal processors, adding an extra high-pass filter (R2 and C2) to remove both the amplified DC offset signal of INA and the electrode polarization mismatch is recommended.

To obtain both modulus and phase of the measured impedance, at the second stage of the signal processing is used a complete four-quadrant, voltage output analog multiplier (MUX), shown as $MULT_1$ in Fig. 8. Using a MUX is the simplest method for having a precise and real-time impedance measurement converted into digital. The key point of a MUX is its transfer function ($=V_{INA}*V_{GAIN}*G_{LOOP}$), where R4 and R5 define the loop gain and V_{GAIN} allows a fine gain tuning by the microcontroller. Even this signal processing is precise and accurate, the output voltage V_{out} contains a DC level which, in turn, is removed by the high-pass filter formed by C_3 and R_3.

Instead of using MUX, one can digitize the INA output voltage directly by an AD converter, then process the signal for extracting both modulus and phase of the material impedance under study. However, if the impedance modulus is the only figure required, then a wide-bandwidth active rectifier and a second-order active filter will do the job. On the other hand, if the impedance phase is the only variable to be evaluated in the impedance spectra, a phase-retrieve circuit can be used, such as a simple multiplier and a second-order active low-pass filter.

Measuring modulus and phase accurately across a load in a wide bandwidth is quite difficult, as parasite capacitance degrades the signal. Therefore, most BIA designs measure the current flow in the load by using a shunt resistor connected in series with the load. The main advantage of measuring the load current is to compensate for the phase shift errors due to stray and cable capacitance, which, in the end, increases the accuracy of the measured biological impedance. Most current-measuring circuits use a trans-impedance amplifier (TIA), composed of a buffer and a differential amplifier. TIA has the advantage of not using an external resistor in series with the load, increasing the voltage swing of the MHCS. On the other hand, using a shunt resistor does not intercept the current return path avoiding errors produced by the TIA, then maintaining the ground reference [19].

A practical circuit for measuring the current flow through the *Load* is shown in Fig. 9. It uses a shunt resistor R_1, a high input impedance buffer (OA_1) for neglecting leakage current, a differential amplifier (OA_2), and a voltage reference of 1.66 V, for example, to centralize the V_S into the dynamic range of the ADC.

It is also recommended that both modulus and phase of load current I_{Load} be measured to calculate the load's impedance more accurately. That measurement can be performed by a MUX, as explained above. Then, both modulus and phase of I_{Load} ($=V_{1.66}/R_1 - V_S/R_1$), assuming $R_2 = R_3 = R_4 = R_5$, are used to calculate the biological load under study. It is important to emphasize that both V_S across the load and shunt resistor are frequency-dependent, then care should be taken when doing such a calculation. Generally, the impedance modulus is then calculated by the ration $|V_{out}|/|I_{Load}|$, whereas the phase by the difference between $\phi Vout$ and $\phi Load$.
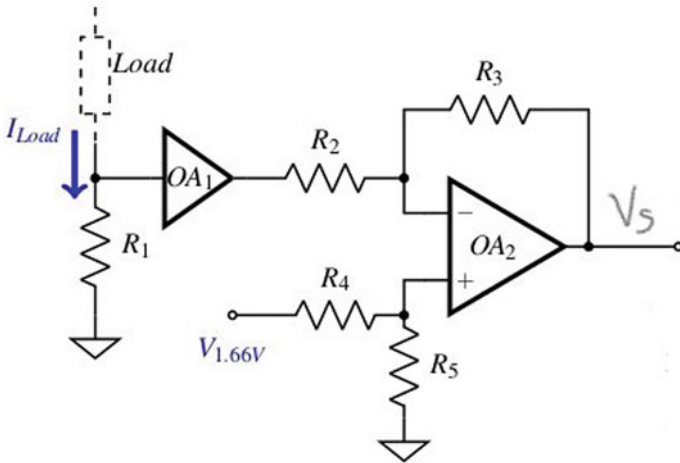
Fig. 9 Schematic diagram of a practical current measuring circuit across the load understudy

3 Extracting Glucose from BIA

BIA technique is a non-invasive method, as already discussed in the above sections, which can be employed to detect blood glucose. BIA is a type of technology considered "transdermal," however other technologies have also been used. They can be divided into different sub-technologies, as shown in Fig. 10. Depending on the environment and the accessed body place for measurements, every technology has its
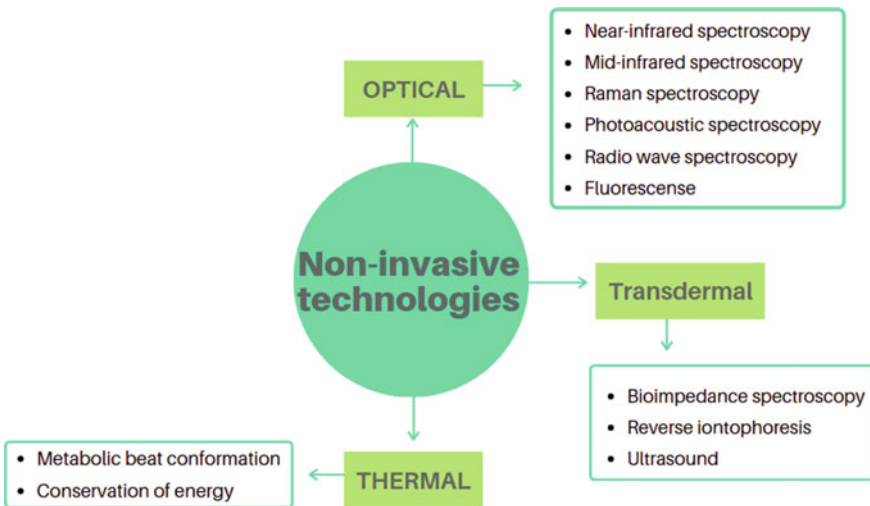

Fig. 10 Diagram showing the most of non-invasive blood measuring technologies

working features, advantages, and disadvantages. For example, transdermal is very sensitive to environmental variables such as temperature or sweating [20]. Optical methods depend on the properties of the tissue, such as color tone in the case of skin [21]. Over the last 10 years, relevant technologies have been launched in the market, such as GlucoWatch® G2 Biographer, Pendra®, OrSense NBM-200G, and Glucose. However, some are not precise enough to predict blood glucose levels, and others were removed from the FDA (USA) market. This chapter presents the solution using only the electrical bioimpedance (also called electrical bioimpedance spectroscopy—EBIS).

Monitoring glucose has been a classic area of research in BIA. Over time, accuracy has been increased but not enough to have clinically acceptable results [22, 23]. Recent studies have presented BIA as a promising non-invasive technique for detecting glucose in the blood [24, 25]. However, it is difficult to choose a proper body site to connect the electrodes because it depends on electrode geometry, circuitry topology, measuring technique, etc.

Glucose can be found in interstitial fluids, and most researchers use it to set up the system [26, 27]. Interstitial fluids are present in every tissue as a component of the extracellular fluids. Interstitial glucose concentration is well correlated with blood glucose concentration, but glucose's appearance in interstitial fluids is delayed compared to it in the blood [28, 29]. Nevertheless, many researchers consider this delay a positive point to glucose monitors because they are more accurate than plasma laboratory analysis. Interstitial glucose is the real glucose that tissue cells use for their metabolism. Blood glucose can eventually exhibit some peaks while interstitial glucose keeps stable. Making insulin corrections during the fake glucose peaks can negatively impact glucose levels because glucose levels do not need to be reduced [30, 31].

Predicting blood glucose by using the spectra of both impedance modulus and phase requires a good analytical or numerical model to be computed. This type of processing deals with measuring exogenous variables (modulus and phase) correlated with variable to be predicted, and modeling how these variables produce effects in variable to be predicted. In addition, if a tissue characterization is required, bioimpedance spectra are necessary to properly extract tissue properties, such as intra- and extracellular components and membrane capacitance. We have seen here that these properties are calculated using a fractal model, shown in [7], containing at least four variables to be fitted over the measured frequency range. The Multiple Linear Regression (MLR) method has been used quite successfully for simple cases with single dispersion materials. When it comes either with complex materials or large data to be processed, other different models have been used for that purpose, such as Support Vector Regression (SVR) and Artificial Neural Network (ANN).

MLR is a linear modeling method that uses the linear relation between a dependent variable and many independent variables. The MLR algorithm has been used to predict blood glucose non-invasively, such as the one that uses the metabolic energy conservation technique [32]. In contrast, the presented by [33] used multiple measured data (capacitive fringing field sensors, optical sensors, and skin hydration

levels). MLR can be used by modeling the blood impedance modulus or phase concerning glucose level measured in milligrams per deciliter (mg/dL).

While linear regression minimizes the error between the actual and predicted values through the line of best fit, SVR manages to fit the best line within a threshold of values, otherwise called the epsilon-insensitive tube. It uses the same basic idea as Support Vector Machine (SVM), but applies it to predict real values rather than a class. It also acknowledges the presence of non-linearity in the data and provides a proficient prediction model. Some SVR applications for blood glucose non-invasively prediction are pulse glucometer [34] and electrochemical measurement of saliva [35]. It can also be used in other re- related areas such as blood glucose level prediction using daily diet information, exercise, and past blood glucose measurements [36]. Most BIA systems measure over 30 discrete frequency points either for modulus or phase, then end up with a large amount of data, especially if other biosignals are also acquired to predict the blood glucose level better.

Handling a large amount of data means dealing with many input data, where an ANN is highly recommended. The more data fed into the network, the more generalized and accurate the predictions are. ANN systems can learn system behaviors using examples to model them without any specific programming or knowledge about the system. It can be used for linear and non-linear problems. ANN has been widely used to predict blood glucose levels non-invasively together with other types of technologies, such as NIRS [37], palm sweat [38], or multisensor systems including photoplethysmogram, heart rate, galvanic skin response and temperature measurements [39]. Another application where ANNs have been used related to glucose is predicting future glucose levels in different time intervals [40].

4   New Trends for Diabetic's Meter

Many studies are trying to deal with the problem of separating the sources producing similar physiological effects as the glucose builds. The use of different sensor technologies helps in this task. Two physiological impacts can have the same behavior: producing thermal effects but different producing coloring effects. The combination ultrasonic, electromagnetic, and thermal has shown an increment of accuracy [41]. Mid-infrared spectroscopy and photoacoustic detection are examples where combining different technologies improves the results compared with using a single technology [42].

When the information comes from multiple sensors, computational algorithms may be used to analyze this information as a set. A neural network has shown a good performance combining near-infrared spectroscopy (NIRS) and bioimpedance analysis (BIA) measurements [24]. Photoplethysmogram, galvanic skin response, and temperature measurements can be combined using multiple linear regression and an artificial neural network to estimate blood glucose levels [39].

Novel approaches have been using nanoparticles as non-enzymatic biosensing of glucose [43] and graphene nanocomposite acting as a non-invasive sensor for measuring blood glucose in diabetic patients [44].

5 Conclusion

It can be resumed that even the Self-Monitoring Blood Glucose (SMBG) market is stabilized using invasive methods, there is a big research gap and enormous interest in the development of non-invasive SMBG devices. It was shown in this chapter that:

i. Current technologies suffer from a lot of problems such as the lack of accuracy and disturbances;
ii. Bioimpedance (BIA) technique has been showing a robust, low cost, and promising technique for tissue characterization and then also to blood glucose estimation;
iii. The use of BIA together with NIR has already proven to be a more accurate joint technique for blood glucose estimation;
iv. Combining multi-sensor measurements with algorithms seems to be a way forward to more accurate glucose estimations in diabetic patients.

Some future outlooks for the non-invasive SMBBG may include the use of biosensors highly sensitive to specific ions or other substances when a patient undergoes a glycemia peak; the use of a multi-agent sensor network for real-time monitoring; the use of AI together with wireless sensors for long term and home care applications.

References

1. Kennelly, A.E.: Impedance. Trans. Am. Inst. Electr. Eng. **10**, 172–232 (1983)
2. Dorf, R.C.: Introduction to electric circuits. Eur. J. Eng. Educ. **18**(4), 430 (1993)
3. Abtahi, F.: Aspects of electrical bioimpedance spectrum estimation. Thesis, Royal Institute of Technology (2014)
4. Fortney, S.M., Nadel, E.R., Wenger, C.B. et al.: Effect of blood volume on sweating rate and body fluids in exercising humans. J. Appl. Physiolo. **51**(6) (1981)
5. Dean, D., Ramanathan, T., Machado, D., et al.: Electrical impedance spectroscopy study of biological tissues. J. Electrostat. **66**(3–4), 165–177 (2008)
6. Bertemes-Filho, P.: Tissue Characterisation using an Impedance Spectroscopy Probe. University of Sheffield, Thesis (2002)
7. Cole, K.: Permeability and Impermeability of cell membranes for ions. Cold Spring Harb. Symp. Quant. Biol. **8**, 110–122 (1940)
8. Sasaki, K., Wake, K., Watanabe, S.: Development of best fit Cole-Cole parameters for measurement data from biological tissues and organs between 1 MHz and 20 GHz. Radio Sci. **49**, 459–472 (2014)

9. Pliquett, U., Barthel, A.: Interfacing the AD5933 for bio-impedance measurements with front ends providing galvanostatic or potentiostatic excitation. J. Phys. Conf. Ser. (407), 012019 (2019)

10. Ferreira, J., Seoane, F., Lindecrantz, K.: AD5933-based electrical bioimpedance spec- trometer. Towards textile-enabled applications. In: Paper presented at the Annual International Conference of the IEEE Engineering in Medicine and Biology Society, Boston, MA, USA, 30 Aug–3 Sept 2 (2011)

11. Mascarenas, D.L., Todd, M.D., Park, G., et al.: Development of an impedance-based wireless sensor node for structural health monitoring. Smart Mater. Struct. **16**(6), 2137–2145 (2007)

12. Margo, C., Katrib, J., Nadi, M., et al.: A four-electrode low frequency impedance spectroscopy measurement system using the AD5933 measurement chip. Physiol. Meas. **34**(4), 391–405 (2013)

13. Sanchez, B., Vandersteen, G., Bragos, R. et al.: Basics of broadband impedance spectroscopy measurements using periodic excitations. Measur. Sci. Technol. **23**(10), 105501 (2012)

14. Sheingold, D.H.: Impedance & admittance transformations using operational amplifiers. Lightning Empiricist **12**(1), 1–8 (1964)

15. Lu, L.: Aspects of an electrical impedance tomography spectroscopy (EITS) system. University of Sheffield, Thesis (1995)

16. Seoane, F., Bragos, R., Lindecrantz, K.: Current source for multifrequency broadband electrical bioimpedance spectroscopy systems—a novel approach. In: Paper presented at the International Conference of the IEEE Engineering in Medicine and Biology Society, New York, United States, 30 Aug–3 Sept 2006

17. Zarafshani, A., Bach, T., Chatwin, C. et al.: Current source enhancements in electrical impedance spectroscopy (EIS) to cancel unwanted capacitive effects. In: Paper presented at the SPIE Medical Imaging, Orlando, Florida, United States, 11–16 Feb 2017

18. Bertemes-Filho, P., Felipe, A., Vincence, V.C.: High accurate howland current source: output constraints analysis. Circuits Syst. **4**, 451–458 (2013)

19. Regan, T., Munson, J., Zimmer, G. et al.: AN105—current sense circuit collection making sense of current. https://www.analog.com/en/app-notes/an-105fa.html. Accessed 13 May 2021

20. Dudukcu, H.V., Yildirim, T.: Noninvasive glucose measurement for diabetes mellitus patients— mini-review. Curr. Trends Biomed. Eng. Biosci. **2**(3), 38–40 (2017)

21. Lister, T., Wright, P.A., Chappell, P.H.: Optical properties of human skin. J. Biomed. Opt. **17**(9), 0909011 (2012)

22. Lupa, P.B., Bietenbeck, A., Beaudoin, C., et al.: Clinically relevant analytical techniques, organizational concepts for application and future perspectives of point-of-care testing. Biotechnol. Adv. **34**(3), 139–160 (2016)

23. Batra, P., Tomar, R., Kapoor, R.: Challenges and trends in glucose monitoring technologies. In: Available via AIP Conference Proceedings. https://aip.scitation.org/doi/ https://doi.org/10.1063/1.4942742. Accessed 13 May 2021

24. Song, K., Ha, U., Park, S., et al.: An impedance and multi-wavelength near-infrared spectroscopy IC for non-invasive blood glucose estimation. IEEE J. Solid-State Circuits **50**(4), 1025–1037 (2015)

25. Liu, Y., Xia, M., Nie, Z., et al.: In vivo wearable non-invasive glucose monitoring based on dielectric spectroscopy. In: Paper presented at the 13th International Conference on Signal Processing, Chengdu, China, 6–10 Nov 2016

26. Zierler, K.: Whole body glucose metabolism. Am. J. Physiol. **276**(3), E409–E426 (1999)

27. Cobelli, C., Dalla Man, C., Sparacino, G., et al.: Diabetes: models, signals, and control. IEEE Rev. Biomed. Eng. **2**, 54–96 (2009)

28. Baek, Y.H., Jin, H.Y., Lee, K.A. et al.: The correlation and accuracy of glucose levels between interstitial fluid and venous plasma by continuous glucose monitoring system. Korean Diabetes J. **34**, 350–358 (2010)

29. Thennadil, S.N., Remmert, J.L., Wenzel, B.J., et al.: Comparison of glucose concentration in interstitial fluid, and capillary and venous blood during rapid changes in blood glucose levels. Diabetes Technol. Ther. **3**(3), 357–365 (2001)

30. Cengiz, E., Tamborlane, W.V.: A tale of two compartments: interstitial versus blood glucose monitoring. Diabetes Technol. Ther. **11**(S1), 11–16 (2009)
31. Kulcu, E., Tamada, J.A., Reach, G., et al.: Physiological differences between interstitial glucose and blood glucose measured in human subjects. Diabetes Care **26**(8), 2405–2409 (2003)
32. Zhu, J., Chen, Z.: Research on the multiple linear regression in non-invasive blood glucose measurement. Bio-Med. Mater. Eng. **26**(S1), 447–453 (2015)
33. Huber, D., Falco-Jonasson, L., Talary, M. et al.: Multi-sensor data fusion for non-invasive continuous glucose monitoring. In: Paper presented at the 10th International Conference on Information Fusion, Québec, Canada, 9–12 July 2007
34. Ogawa, M., Yamakoshi, Y., Satoh, M., et al.: Support vector machines as multivariate calibration model for prediction of blood glucose concentration using a new non-invasive optical method named pulse glucometry. IEEE Trans. Biomed. Eng. **54**(3), 571–572 (2007)
35. Malik, S., Khadgawat, R., Anand, S., et al.: Non-invasive detection of fasting blood glucose level via electrochemical measurement of saliva. Springerplus **5**(1), 701 (2016)
36. Bunescu, R., Struble, N., Marling, C. et al.: Blood glucose level prediction using physiological models and support vector regression. In: Paper presented at the 12th International Conference on Machine Learning and Applications, Miami, United States, 4–7 Dec 2013
37. Ramasahayam, S., Koppuravuri, S.H., Arora, L., et al.: Noninvasive blood glucose sensing using near infra-red spectroscopy and artificial neural networks based on inverse delayed function model of neuron. J. Med. Syst. **39**(1), 166 (2015)
38. Saraoğlu, H.M., Koçan, M.: A study on non-invasive detection of blood glucose concentration from human palm perspiration by using artificial neural networks. Expert. Syst. **27**(3), 156–165 (2010)
39. Yadav, J., Rani, A., Singh,, V. et al.: Investigations on multisensor-based noninvasive blood glucose measurement system. J. Med. Devices **11**(3), 031006 (2017)
40. Pérez-Gandía, C., Facchinetti, A., Sparacino, G., et al.: Artificial neural network algorithm for online glucose prediction from continuous glucose monitoring. Diabetes Technol. Ther. **12**(1), 81–88 (2010)
41. Harman-Boehm, I., Gal, A., Raykhman, A.M., et al.: Noninvasive glucose monitoring: increasing accuracy by combination of multi-technology and multi-sensors. J. Diabetes Sci. Technol. **4**(3), 583–595 (2010)
42. Kottmann, J., Rey, J.M., Sigrist, M.W.: Mid-infrared photoacoustic detection of glucose in human skin: towards non-invasive diagnostics. Sensors (Basel) **16**(10), 1663 (2016)
43. Dayakar, T., Venkateswara, K., Parkb, J., et al.: Non-enzymatic biosensing of glucose based on silver nanoparticles synthesized from Ocimum tenuiflorum leaf extract and silver nitrate. Mater. Chem. Phys. **216**, 502–507 (2018)
44. Yempally, S., Hegazy, S.M., Aly, A., et al.: Non-Invasive diabetic sensor based on cellulose acetate/graphene nanocomposite. Macromol. Symp. **392**, 1–5 (2020)

Pedro Bertemes-Filho Graduated in Electrical Engineering in 1995 at the State University of Santa Catarina and Ph.D. in Medical Physics at the University of Sheffield. Awarded by Fulbright at Dartmouth College and visiting researcher in the University of Ljubljana. Titular Professor at UDESC since 2004, lecturing electronic instrumentation, sensors and transducers, introduction on biomedical engineering and coordinating research groups in biomedical engineering and electrical bioimpedance. Senior IEEE member since 2020. Reviewer of more than 12 international journals. Secretary of the ISEBI from 2019 to 2022. International lectures in renowned Universities, such as Uruguay, Ljubljana, Sheffield, Copenhagen and Mexico. Areas of research interest are focused on electrical bioimpedance and bioinstrumentation, Biosensor and e-Health. Edited international books, such as "Bioimpedance in Biomedical Applications and Research" and "Medicine-Based Informatics and Engineering" by Springer.